Total chemical synthesis and high-resolution crystal structure of the potent anti-HIV protein AOP-RANTES

Jill Wilken[1]*, David Hoover[2]*, Darren A Thompson[1], Paul N Barlow[3], Helen McSparron[3], Laurent Picard[4], Alexander Wlodawer[2], Jacek Lubkowski[2] and Stephen BH Kent[1]

Background: RANTES is a CC-type chemokine protein that acts as a chemoattractant for several kinds of leukocytes, playing an important pro-inflammatory role. Entry of human immunodeficiency virus-1 (HIV-1) into cells depends on the chemokine receptor CCR5. RANTES binds CCR5 and inhibits HIV-1 entry into peripheral blood cells. Interaction with chemokine receptors involves a distinct set of residues at the amino terminus of RANTES. This finding was utilized in the development of a chemically modified aminooxypentane derivative of RANTES, AOP-RANTES, that was originally produced from the recombinant protein using semisynthetic methods.

Results: AOP-RANTES has been produced by a novel total chemical synthesis that provides efficient, direct access to large amounts of this anti-HIV protein analog. The crystal structure of chemically synthesized AOP-RANTES has been solved and refined at 1.6 Å resolution. The protein is a dimer, with the amino-terminal pentane oxime moiety clearly defined.

Conclusions: Total chemical synthesis of AOP-RANTES provides a convenient method of producing the multi-milligram quantities of this protein needed to investigate the molecular basis of receptor binding and antiviral activity. This work provides the first truly high-resolution structure of a RANTES protein, although the structure of RANTES was known from previous nuclear magnetic resonance (NMR) determinations.

Addresses: [1]Gryphon Sciences, 250 East Grand Avenue, Suite 90, South San Francisco, CA 94080, USA. [2]Macromolecular Structure Laboratory, ABL-Basic Research Program, NCI-FCRDC, Frederick, MD 21702, USA. [3]Edinburgh Centre for Protein Technology, The University of Edinburgh, Joseph Black Chemistry Building, The King's Buildings, West Mains Road, Edinburgh, EH9 3JJ, UK. [4]INSERM U.332, Institut Cochin de Génétique Moléculaire, 22 rue Méchain, 75014 Paris, France.

*Contributed equally to this work

Correspondence: Stephen BH Kent or Jacek Lubkowski
E-mail: steve_kent@gryphon.com or jacek@ncifcrf.gov

Key words: chemical protein synthesis, chemokine, crystal structure, HIV-1, RANTES

Received: **10 September 1998**
Revisions requested: **12 October 1998**
Revisions received: **2 November 1998**
Accepted: **9 November 1998**

Published: **21 December 1998**

Chemistry & Biology January 1999, 6:43–51
http://biomednet.com/elecref/1074552100600043

 ISSN 1074-5521

Introduction

Chemokines are a diverse family of numerous small (8–10 kDa) proteins that mediate a wide range of inflammatory responses in humans. These proteins are secreted at the site of injury by many types of tissue cells, including platelets, and frequently act as chemoattractants for a variety of blood cells. Chemokines display a conserved pattern of cysteine residues and are categorized into two major subgroups, CC and CXC, depending on the sequence of two key cysteine residues near the amino terminus of the proteins. RANTES (regulated on activation normal T cell expressed and secreted) is a 9 kDa CC chemokine protein that acts as a chemoattractant and activating agent for a broad range of immune system cells, such as monocytes, T lymphocytes and eosinophils, but not neutrophils [1]. It is suggested to play a role in certain inflammatory disorders, such as endotoxemia [2] and rheumatoid arthritis [3]. RANTES binds to and signals through a number of chemokine receptors, namely CCR1 [4–8], CCR3 [7], CCR4 [9] and CCR5 [10–12]. Other CC chemokines, such as MIP-1α and MIP-1β, can compete for binding to each of the RANTES receptors. This competition is not surprising, as their amino-acid sequences and tertiary structures are quite similar. Because cells possess more than one type of chemokine receptor, a complicated modulation of effects can arise by the cross-networking of receptors and chemokine ligand interactions.

The chemokine receptor CCR5 is a seven-transmembrane G-protein-coupled receptor that has been identified as the principal coreceptor for human immunodeficiency virus-1 (HIV-1) entry into peripheral blood cells. Because CCR5 acts as a coreceptor for HIV-1 uptake into mononuclear cells, the binding of RANTES to CCR5 and the subsequent internalization of the chemokine–receptor complex can block the initial infection by the virus [13,14]. Recently, it was shown that chemical modification of RANTES at the amino terminus produced a potent antagonist of HIV-1 entry into macrophages and other peripheral blood lymphocytes mediated by CCR5 [15]. In that work, based on the observation that Met-RANTES (a derivative of RANTES in which a methionine residue precedes the normal amino-acid sequence) acted as a receptor antagonist, the protein AOP-RANTES was prepared from recombinantly expressed

Figure 1

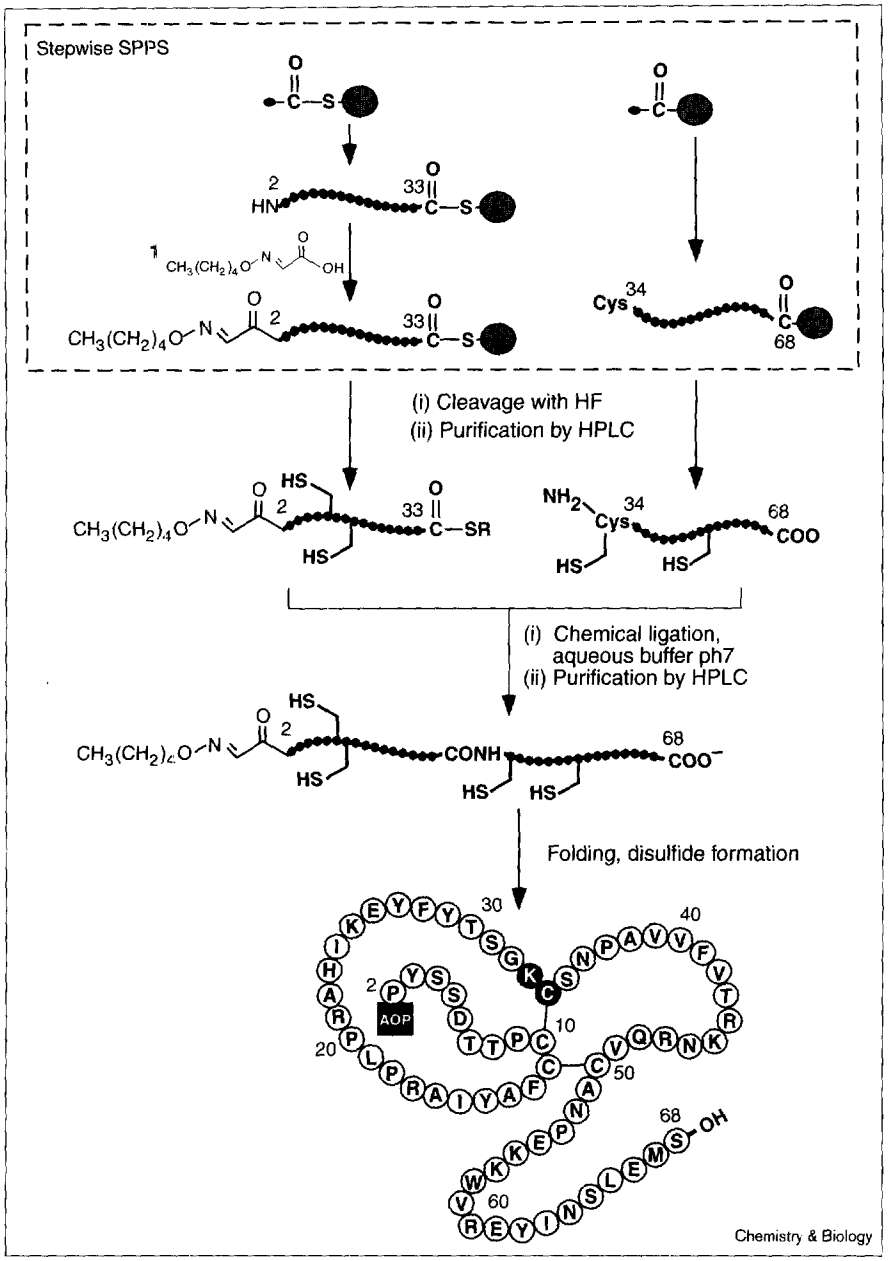

Synthetic scheme for the preparation of AOP-RANTES by means of native chemical ligation of unprotected peptide in aqueous solution. The two shaded residues show the native chemical ligation site at Lys33–Cys34. Single-letter amino-acid code is used.

RANTES by semisynthetic methods [16]. Mild periodate oxidation of the 1-amino 2-ol moiety in the amino-terminal serine of the folded disulfide-containing RANTES protein molecule generated a glyoxal functionality; subsequent chemoselective reaction with aminooxypentane was used to form an oxime bond, generating the modified protein [n-pentyl-O-N = CHCO][*des*Ser^1]RANTES [15].

Here, we report a novel total chemical synthesis that provides more efficient, direct access to large amounts of AOP-RANTES. In a retrosynthetic sense, AOP-RANTES was first envisioned as the unfolded polypeptide chain, which was, in turn, divided into an amino-terminal segment, the peptide AOP-RANTES (2–33)-α-thioester and a carboxy-terminal segment, RANTES (34–68). This approach allowed us to use native chemical ligation [17] to join these unprotected peptide segments at the central Lys33–Cys34 sequence by reaction in aqueous solution at neutral pH (Figure 1). After preliminary experimentation, we devised a practical route for the incorporation of the AOP moiety, and the amino-terminal segment was further retrosynthetically divided into the peptide moiety comprising residues 2–33 and the oxime-containing moiety (compound **1**, Figure 1) to provide a practical route to the desired protein molecule.

We used the resulting high-purity chemically synthesized AOP-RANTES protein for X-ray crystallography to determine the three-dimensional structure of the molecule.

The structure of recombinant RANTES in solution was previously determined independently by two groups [18,19], but many questions about the structure were left unanswered in these medium-quality nuclear magnetic resonance (NMR) studies. Specifically, the positions of the first five residues of the amino terminus and several of the residues at the carboxyl terminus were not defined at all, and the orientation of the two monomers within the dimer was not well defined. In this paper, we report the use of X-ray crystallography to reveal the structure of a RANTES protein in much greater detail. The majority of the structure remains similar to the NMR models, as shown by comparison to the high-resolution (1.6 Å) crystal structure of AOP-RANTES described here. Furthermore, in electron-density maps of the crystalline protein, the amino terminus of AOP-RANTES is clearly bound in a hydrophobic depression on the surface of the protein molecule.

Results and discussion

Chemical synthesis of the AOP-RANTES (2–68) polypeptide

Synthesis of the peptide segments was accomplished in a straightforward manner using stepwise solid phase peptide synthesis (SPPS) [20]. The amino-terminal segment AOP-RANTES (2–33)-α-thioester was prepared on a thioester-generating resin [21], using highly optimized Boc chemistry SPPS [22]. At the last step in the synthesis of this segment, the modified amino terminus was generated by on-resin reaction of RANTES (2–33) with compound **1** preactivated as the HOAt (1-hydroxy-7-azabenzotriazole) ester to give AOP-RANTES (2–33)-α-thioester-resin. This reaction proceeded quantitatively, with none of the starting material RANTES (2–33) detected by electrospray ionization–mass spectrometry (ESI–MS) after cleavage and deprotection. Several other routes for the incorporation of the oxime moiety were also explored, but with unsatisfactory results. Synthesis of the carboxy-terminal peptide segment RANTES (34–68) was carried out according to published protocols [22]. Both peptide segments were synthesized on a 0.25 mmol scale of starting aminoacyl-resin. Following deprotection and cleavage (anhydrous hydrogen fluoride, *p*-cresol (5% v/v), 0°C, 1 h), the peptides were purified using reverse-phase high-pressure liquid chromatography (RP–HPLC) in good yield: greater than 100 mg quantities of each purified segment were obtained from a single synthesis.

AOP-RANTES (2–33)-α-thioester (25 μmol) and RANTES (34–68) (27 μmol) were reacted at pH 7 in aqueous buffer containing 6 M GuHCl as a chaotropic agent. Thiophenol (0.5% v/v) was added to the ligation mixture to ensure that cysteine residues were present in the reduced form and to catalyze the reversal of unproductive thioester formation

Figure 2

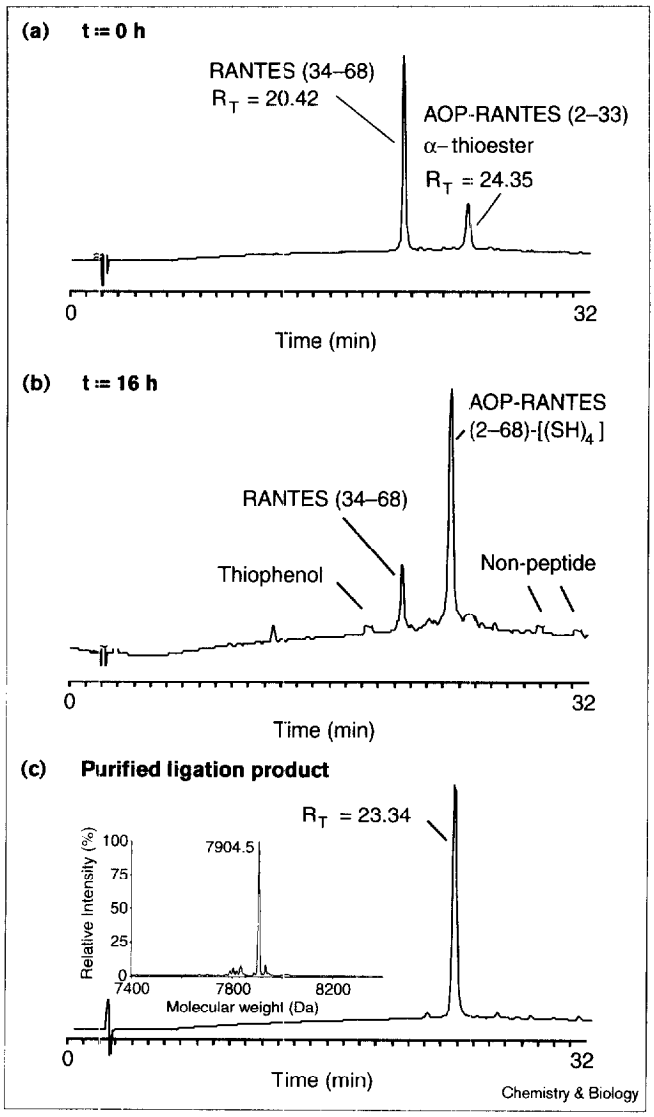

Native chemical ligation of AOP-RANTES (2–33)-α-thioester and RANTES (34–68) in aqueous solution at pH 7. The ligation reaction is shown at: **(a)** 0 and **(b)** 16 h. The ligation reaction was monitored by injecting 1 μl aliquots of the ligation solution on a C4 RP–HPLC column with a gradient of 5–65% acetonitrile versus water containing 0.1% TFA, over 30 min. Detection was at 214 nm. **(c)** Characterization of the purified ligation product. Analytical RP–HPLC chromatogram with an inset showing ESI–MS of AOP-RANTES (2–68)-[(SH_4)]: observed mass, 7904.5 ± 0.6 Da; calculated mass (average isotope composition), 7905.1 Da.

[23]. The amino-terminal segment, AOP-RANTES (2–33)-α-thioester, was added in portions to minimize insolubility due to aggregation and consequent poor reaction. The ligation reaction was monitored using analytical RP–HPLC and ESI–MS and was shown to have gone to completion after 16 h (Figure 2b). No significant side reactions were observed for ligation using this functionalized peptidyl-lysine-α-thioester (Figure 2). Purification of the ligation

Figure 3

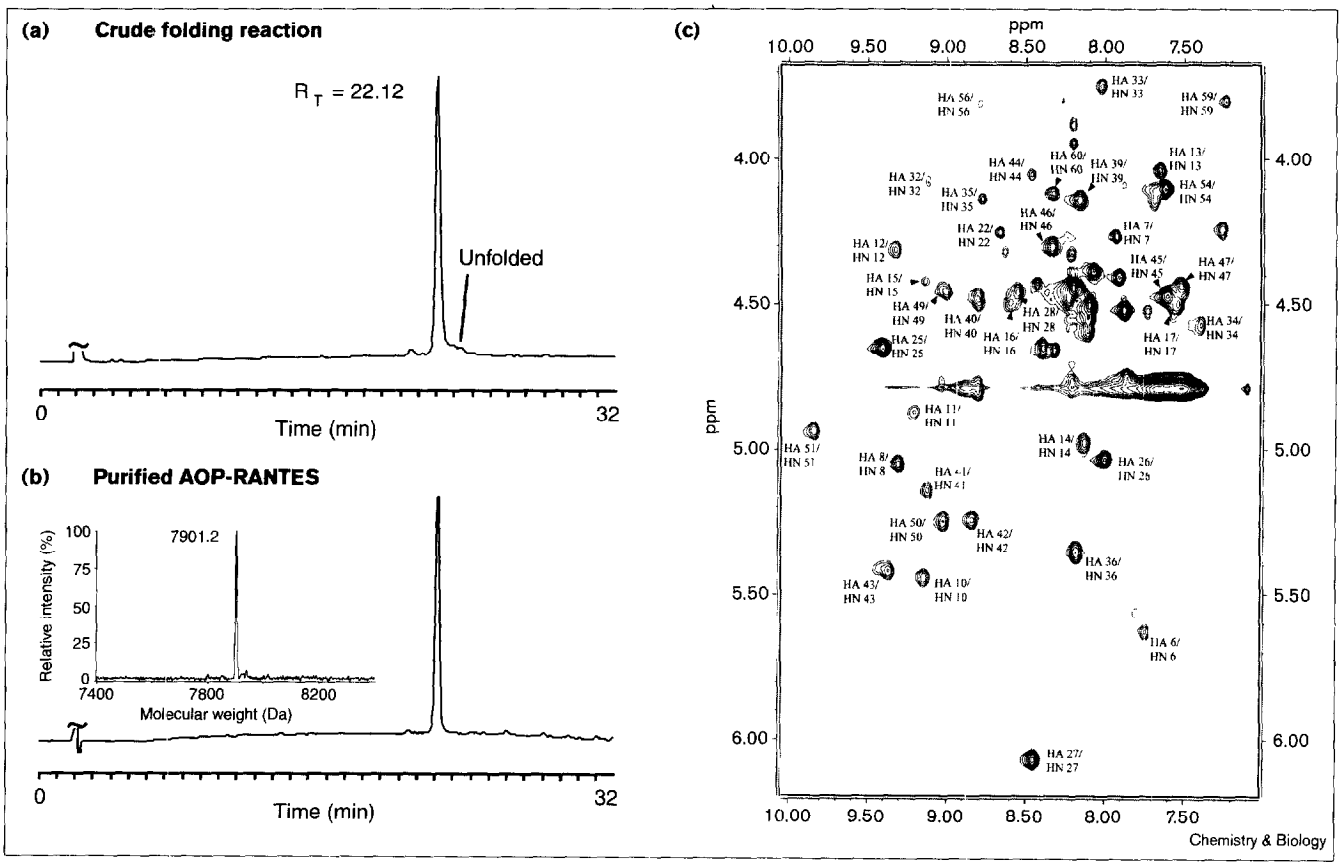

Folding/disulfide formation. The purified polypeptide AOP-RANTES (2–68)-[$(SH)_4$] was stirred overnight at pH 8 in 2 M GuHCl in the presence of 8 mM cysteine and 1 mM cystine. **(a)** Analytical RP–HPLC chromatogram of the total crude folding products obtained. For the major product, the retention time is 1.22 min earlier than the reduced polypeptide, which is consistent with folding/disulfide formation. **(b)** Characterization of purified synthetic AOP-RANTES. Analytical RP–HPLC chromatogram with an inset showing ESI–MS of AOP-RANTES: observed mass, 7901.2 ± 0 6 Da; calculated mass (average isotope composition), 7091.15 Da. **(c)** ^1H NMR measurements on the synthetic protein AOP-RANTES (two-dimensional TOCSY experiment performed at 600 MHz). The data show that a single conformation predominates and are consistent with the canonical chemokine fold. The annotations refer to the backbone assignments made on this sample.

solution by semipreparative RP–HPLC gave the ligated polypeptide product AOP-RANTES (57.8 mg, 7.3 μmol, 30% recovered yield based on peptide segments). The yield is significantly reduced compared with similar chemical-ligation synthesis of native RANTES, which may be attributed to reduced recovery in the reversed-phase purification due to the increased hydrophobicity of the AOP-polypeptide. The reduced polypeptide was characterized by ESI–MS (observed mass, 7904.5 ± 0.6 Da; calculated mass, average isotope composition, 7905.2 Da).

Folding and characterization

Folding and disulfide formation was carried out at pH 8 by dissolving the purified polypeptide AOP-RANTES (2–68)-[$(SH)_4$] in an aqueous buffer of 2 M GuHCl, 100 mM Tris containing 8 mM cysteine and 1 mM cystine. After gentle stirring overnight, near-quantitative folding was obtained (Figure 3a). Compared with the reduced polypeptide chain, the folded product gave a sharp peak that eluted earlier on an analytical RP–HPLC column, consistent with the formation of a folded disulfide-cross-linked protein. In comparison with the reduced polypeptide, using ESI–MS, this product showed a loss of 3.3 ± 1.2 mass units, consistent with the formation of the expected two disulfides in the folded protein molecule. Purification by semipreparative RP–HPLC produced the protein AOP-RANTES (32 mg, 4.0 μmol, 55% yield based on unfolded polypeptide, 16% yield based on peptide segments) in greater than 95% purity (as determined by analytical RP–HPLC; Figure 3b). The product was characterized further using ESI–MS (observed mass 7901.2 ± 0.6 Da; calculated mass, average isotope composition, 7901.2 Da).

The correct formation of the protein tertiary structure was confirmed using NMR spectroscopy. Under the conditions used (pH 3.7, ~1 mM protein), native RANTES is mainly a

dimer [18]. As shown in Figure 3c, it was possible to assign, in most cases, single cross-peaks in the total correlation spectroscopy (TOCSY) spectrum to particular residues of AOP-RANTES, demonstrating that a single conformation predominates. Some evidence of a second conformation is present, but this is also seen for the native RANTES and arises from the presence of the monomeric form at low concentration. Moreover, the chemical shifts of assigned residues are nearly identical to those of the equivalent residues in native RANTES, which demonstrates that both proteins have very similar structures. The evidence for correct formation of the protein tertiary structure was further provided by the crystal structure (see below) and by the ability of synthetic AOP-RANTES to completely inhibit CCR5-dependent fusion of HIV-1 M-tropic Env proteins gp120–gp41 with an ED_{50} of ~1 nM in the cell fusion assay using HeLa-CD4-CCR5-LTR*LacZ* and HeLa-Env_{ADA} cell lines (L.P., unpublished observations). In contrast, chemically synthesized RANTES with an unmodified covalent structure had an ED_{50} of > 100 nM in the same assay. These results are consistent with the observations reported using recombinant RANTES and the recombinant-derived semisynthetic AOP-RANTES [15].

Crystal structure of AOP-RANTES

AOP-RANTES prepared by total chemical synthesis was crystallized using the hanging drop method by ammonium-sulfate precipitation from a pH 4.5 solution. Small, high-quality crystals were obtained. The structure of AOP-RANTES was determined at 1.6 Å resolution, using data collected with synchrotron radiation on beamline X9B at the National Synchrotron Light Source (NSLS), Brookhaven National Laboratory. Phases were obtained by molecular replacement using the structure of Met-RANTES (D.H. and J.L., unpublished observations). The positions for all atoms could be defined by electron density, except for the sidechain of Lys45 in monomer B, which has been modeled in two alternate conformations. The amino terminus, from the AOP moiety to residue Thr7, is clearly defined (Figure 4) and packs against the noncrystallographically related monomer, with the AOP group bound within a hydrophobic depression on the surface (Figure 5). The fold of the AOP-RANTES monomer is similar to that of other CC and CXC monomers, forming a three-stranded antiparallel β sheet flanked by a carboxy-terminal α helix (Figure 6). A short β sheet (β1) is formed between the monomers from residues Thr8 to Cys10, finishing with a long loop between Cys11 and Pro20 that stretches over the molecule. After a short 3_{10} helix (Arg21–His23), the main β sheet is formed by Ile24–Tyr29 (β2), Val39–Thr43 (β3) and Gln48–Ala51 (β4). Residues Lys56–Glu66 form the carboxy-terminal α helix (α1), with residues Met67 and Ser68 in an extended conformation. The loop between β2 and β3 contains a type III reverse turn (Ser31–Cys34); the loop between β3 and β4, a distorted type I reverse turn (Thr43–Asn46); and the loop between β4 and α1, a type I reverse turn (Asn52–Lys55). Secondary structure elements were defined using the program DSSP [24].

Figure 4

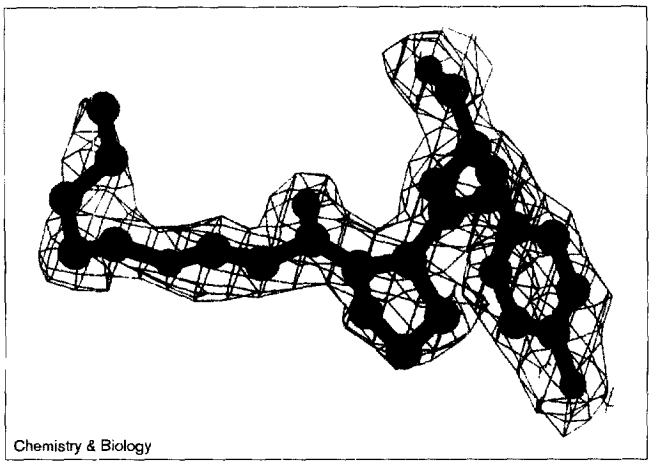

Electron density contoured at 1.2 σ surrounding the AOP group, Pro2 and Tyr3. The figure was made using MOLSCRIPT [39] and Raster3D [40].

The contacts between monomers that are involved in creating the dimer are minimal. Aside from the antiparallel β sheet formed by residues Thr8–Cys10 and the AOP-linked amino termini, hydrogen bonds are formed between Ser5(O) and Cys50′(N), Asp6(N) and Gln48′(O) and Thr7(OG1) and Gln48′(OE1). Also, there are several

Figure 5

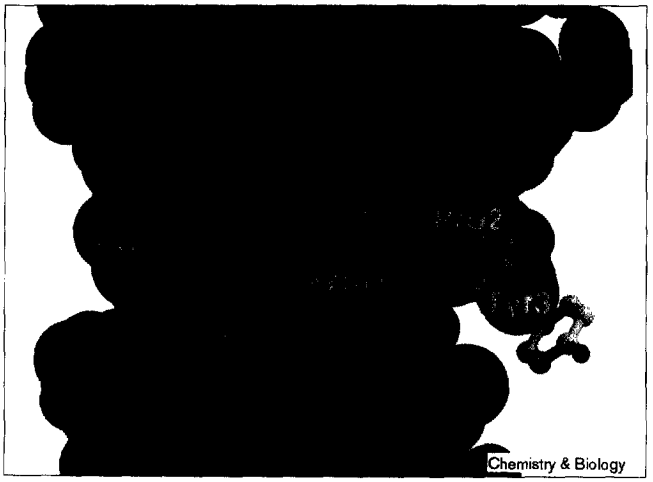

Close-up of the AOP 1 moiety. The AOP group contacts the noncrystallographically related monomer at a hydrophobic depression formed between the phenolic ring of Tyr14, the backbone atoms of Ala13 and Phe12, the Cβs of Cys11, Asn36 and Pro37 and the Cγ of Thr30. The figure was made using MOLSCRIPT [39] and Raster3D [40].

Figure 6

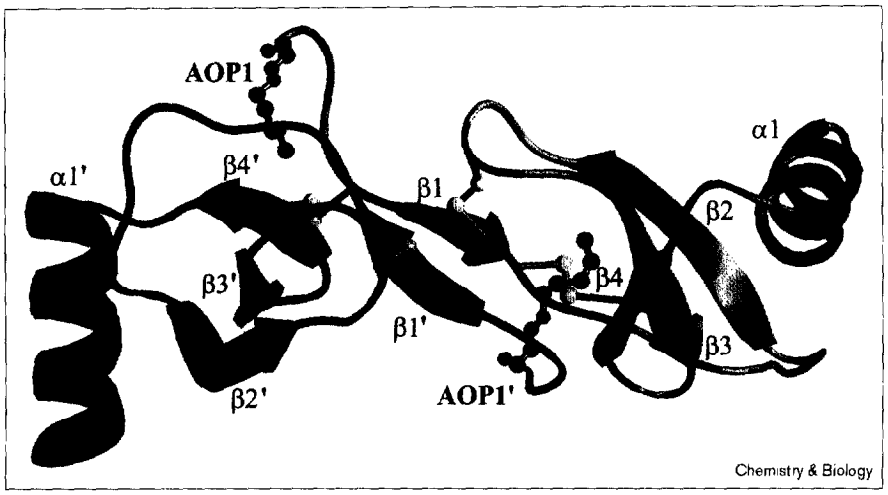

Overall structure of AOP-RANTES. The dimer is shown here as it appears in the asymmetric unit of the crystal structure. Secondary-structure elements as labeled were determined using the program DSSP [24]. The figure was made using the program RIBBONS [41].

solvent-mediated hydrogen-bond bridges across the dimer interface, connecting the loops between β2 and β3. Because of loose packing between the monomers, a gap between Phe12 and Phe12′ is filled with a solvent molecule that alternates between two positions in the crystal.

The conformation of the AOP group, Pro2 and Tyr3 is slightly different in the two monomers. This difference can be explained by a crystal contact in one of the monomers. There are contacts between the peptide Pro2–Tyr3 of monomer B and the symmetry-related ring of Tyr29, which cause the amino terminus to push closer to the protein. There are no contacts between the amino terminus of monomer A and crystallographically related molecules, however. Comparison of the amino termini from both monomers shows the amino terminus of monomer A to be better resolved and more highly ordered than monomer B, with clearer density and lower temperature factors. The crystal contacts of monomer B seem to disrupt the close packing of the AOP group, and the conformation of the AOP group in monomer A suggests an unbiased conformation.

Comparison of AOP-RANTES crystal structure to RANTES NMR structures

There is very little difference in the secondary structure between the crystal structure of AOP-RANTES, described here and the NMR structures of native RANTES [18,19], aside from assignment discrepancies at the ends of secondary structure elements. The root mean square deviation (rmsd) values for superpositioning the backbone atoms of AOP-RANTES residues 10–68 onto the equivalent atoms of the 1RTO [18] and 1HRJ [19] structures are 1.0 and 1.3 Å, respectively. The amino terminus (residues 1–10) moves significantly in the overlay of AOP-RANTES on these NMR structures, however (Figure 7). In contrast to the RANTES NMR structures, in which the conformation of the first five residues was not determined at all and several carboxy-terminal residues are extensively disordered, the AOP group, Pro2 and Tyr3 are seen quite clearly in the AOP-RANTES crystal structure (Figure 4). The amino termini wrap around the neighboring monomer, rather than being more exposed to the solvent. The conformation of the disulfide bridge between Cys10 and Cys34 is different for the AOP-RANTES structure; although this bridge makes a left-handed turn in all three structures, it is slightly distorted in the 1RTO structure [18] and very distorted in the 1HRJ model [19]. Because of the movement of Cys10, changes between the NMR and crystal structures are noticeable in the loop between β2 and β3, probably due to the disulfide link between Cys10 and Cys34. There are also several flipped peptide bonds between residues 31 and 36. Although the hydroxyl group of Thr30 is hydrogen bonded to Ala38(N) in the NMR structures, the donor hydroxyl oxygen is replaced by the carbonyl oxygen of Thr30 in the crystal structures. This replacement buries the sidechain into the protein and allows the loop to pack more tightly against the protein. The differences between the NMR models and the crystal structure might be due, in part, to the relatively small amount of information afforded by the solution spectroscopic protein structure determinations, resulting in insufficient geometric constraints; the flexibility of the protein might also play a role in these differences.

The largest differences are found in the dimer interface. The sparse contacts between the monomers seem to allow the dimer to flex, as seen in a comparison of the AOP-RANTES dimer with the NMR structures of RANTES. This flexibility seems to be inherent to the molecule, because much larger differences between quaternary structures of RANTES were reported in the NMR models [18,19] and in the structures of a related CC chemokine, MCP-1, observed in different crystal forms [25]. Although

the two monomers are linked through a short β sheet by residues Thr8–Cys10, the relative orientations of the monomers to each other are quite different. The dimeric structure of AOP-RANTES is more compact than the NMR structure, as reflected in the total buried surfaces. AOP-RANTES buries 20% of the total monomeric solvent-accessible surface on dimerization (monomer A = 5125 Å^2, monomer B = 4917 Å^2, dimer = 8081 Å^2), whereas the NMR structures bury only 14% in the 1RTO model (monomer A = 5314 Å^2, monomer B = 5316 Å^2, dimer = 9186 Å^2) [18] and 16% in the 1HRJ model (monomer A = 5451 Å^2, monomer B = 5429 Å^2, dimer = 9142 Å^2) [19]. The difference in the buried surface area between AOP-RANTES and RANTES is due mainly to the tight fit between the Pro2 and AOP groups wrapped around the surface of the neighboring monomer. Although it is questionable whether the monomer or dimer is the active form of the molecule, it is known that at physiological pH RANTES can form higher-order oligomers at high concentration [18] and in the presence of glycosaminoglycans [26].

It has been shown in many studies that the amino terminus of RANTES and other CC chemokines plays a crucial role in the binding to and activation of chemokine receptors. Truncations and alterations of the amino terminus give rise to chemokine antagonists of various potency [27–29], as well as inhibiting the infection of primary human macrophages by HIV-1 *in vitro* [15]. Yet the exact role of the AOP group in this effect is not known, but could be due to an increase of affinity for the receptor, a decrease in receptor activation and/or an inhibition of receptor recycling [14,30]; all of these effects would arise from some unknown interaction between the chemokine and the receptor. Another possibility includes a change in transfer to the cell surface as mediated by glycosaminoglycans [26], although the binding to glycosaminoglycans has been shown to be mediated primarily by positively charged residues on a surface far from the amino terminus [31].

The attachment of the AOP moiety to the amino terminus alters the chemical nature and surface features of the RANTES molecule; this could give rise to any of the possible scenarios described above. The crystal structure of AOP-RANTES shows the amino terminus to be clearly defined and bound to the surface as compared with the disordered amino terminus of native RANTES. The sequestration of the amino terminus from solution to the surface might therefore disallow specific interactions with chemokine receptors. Alternatively, the presence of the AOP group might disturb the monomer/dimer equilibrium, which might or might not play a role in receptor binding and activation [32]. Without a complete understanding of chemokine receptor activation, it is difficult to state the reasons for the antagonist properties of AOP-RANTES. Further studies of other RANTES derivatives would be helpful in evaluating different hypotheses. The availability of reliable synthetic methods should facilitate these investigations greatly.

Figure 7

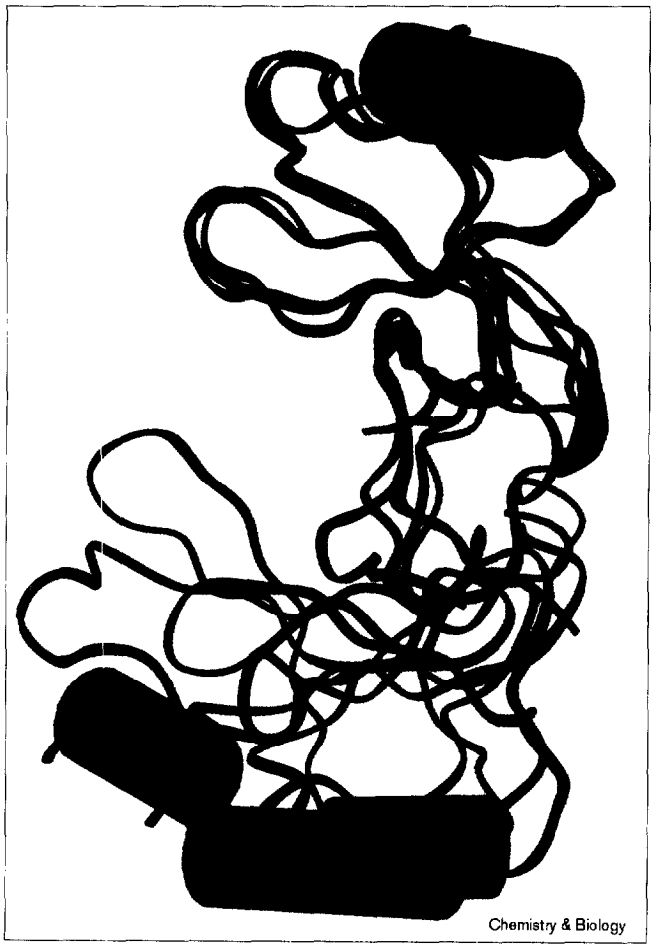

Overlay of the crystal structure of AOP-RANTES on the two available NMR structures of native, recombinant RANTES. As can be seen, the monomer–monomer orientation in the dimer is very different between the crystal structures and the NMR structures. AOP-RANTES is shown in blue, 1RTO [18] in green, and 1HRJ [19] in red. This figure was made using RIBBONS [41].

Significance

In this paper, we have described a convenient total chemical synthesis of high-purity AOP-RANTES on a multi-milligram scale. These large amounts of protein are essential to fully characterize the properties of this potent anti-HIV chemokine derivative in animal models and are necessary for structural analysis using ^{1}H nuclear magnetic resonance (NMR) and X-ray crystallography. The synthetic polypeptide folded to give a homogeneous protein species. The synthetic protein crystallized and diffracted X-rays to high resolution (better than 1.6 Å). The secondary structure of synthetic AOP-RANTES is very similar to that of recombinant RANTES, as shown by

comparison of the crystal structure with NMR structures. Robust synthetic access to modified forms of RANTES will enable the systematic application of the principles of medicinal chemistry to refining the properties of this important protein molecule. Such refinement will be of great value in the search for improved CCR5 receptor antagonists and will facilitate the development of agents to block HIV-1 entry into peripheral blood cells, the primary infective step in AIDS.

Materials and methods

Synthesis of the aminooxypentane-glyoxal oxime **1**

Aminooxypentane TFA salt (550 mg, 2.53 mmol), glyoxylic acid monohydrate (210 mg, 2.28 mmol) and pyridine (410 µl, 5.06 mmol) in methanol (10 ml) were heated under reflux for 2 h. The volatiles were removed *in vacuo* and the resulting oil was extracted with ethyl acetate. Combined extractions were washed with 10% citric acid and water, then dried in the presence of sodium sulfate. The volatiles were removed *in vacuo* to give oxime **1** as a colorless solid.

Synthesis of the peptide segment

Peptides were synthesized using highly optimized Boc SPPS protocols [22]. Boc amino acids were used with the following sidechain protection: Arg(Tosyl), Asn(Xanthyl), Asp(OcHxl), Cys(4MeBzl), Glu(OcHxl), His(DNP), Lys(2ClZ), Ser(Bzl), Thr(Bzl), Trp(formyl) and Tyr(BrZ). AOP-RANTES (2–33)-α-thioester was synthesized on a thioester-generating resin [21] with compound **1** coupled as the preactivated HOAt ester for 5 h at room temperature as the last step in the synthesis. RANTES (34–68) was synthesized on a Boc-Ser(Bzl)OCH_2-Pam resin. After completion of the chain assembly, the peptides were simultaneously cleaved and deprotected from the resin by using anhydrous hydrogen fluoride containing 5% *p*-cresol for 1 h at 0°C. The crude peptides were purified on a C4 RP-HPLC column (linear gradient of 15–55% acetonitrile and H_2O containing 0.1% TFA for 53 min). Fractions were analyzed by ESI–MS, and those of the correct mass were pooled and lyophilized [AOP-RANTES (2–33)-α-thioester: observed mass, 4178.1 ± 0.77 Da; calculated mass, 4178.6 Da (average isotope composition); RANTES (34-68): observed mass, 4098.0 ± 0.50 Da; calculated mass, 4097.8 Da (average isotope composition)].

Synthesis of AOP-RANTES (2–68)-[$(SH)_4$]

RANTES (34–68) (111 mg, 27 µmol) was dissolved in 6 M GuHCl, 200 mM phosphate (pH 7) containing 0.5% thiophenol and ligated with AOP-RANTES (2–33)-α-thioester (104 mg, 25 µmol) at a final peptide concentration of 20 mg ml^{-1}. The ligation reaction was allowed to proceed to completion with stirring for 16 h. Excess 2-mercaptoethanol was added to the ligation solution to reduce partially oxidized ligated product prior to purification on a C4 RP–HPLC column (linear gradient of 20–60% acetonitrile and H_2O containing 0.1% TFA for 60 min). Fractions were analyzed by ESI–MS, and those of the correct mass were pooled and lyophilized [AOP-RANTES (2–68)-[$(SH)_4$]: observed mass, 7904.5 ± 0.4 Da; calculated mass, 7905.2 Da (average isotope composition)].

Folding

AOP-RANTES (2–68)-[$(SH)_4$] was dissolved at 1 mg ml^{-1} in 2 M GuHCl, 100 mM Tris (pH 8) containing 8 mM cysteine and 1 mM cystine. After gentle stirring overnight, the protein solution was purified on a C4 RP–HPLC column (linear gradient of 10–50% acetonitrile and H_2O containing 0.1% TFA for 60 min). Fractions were analyzed using ESI–MS, and those of the correct mass were pooled and lyophilized [AOP-RANTES: observed mass, 7901.2 ± 0.6 Da; calculated mass, 7901.2 Da (average isotope composition)].

NMR Measurements

For NMR experiments, 5 mg of protein was dissolved in 0.54 ml of 25 mM sodium acetate buffer (pH 3.7) containing 60 µl of D_2O. Experiments were conducted at 37°C. To assess the conformational homogeneity of the synthesized protein, a TOCSY experiment was performed using the DIPSI-2 sequence [33], with water suppression by the double pulse field gradient spin echo technique [34]. The mixing time was 40 ms; acquisition times were 70 ms in the first dimension and 170 ms in the second dimension. For each of 512 complex increments, 64 scans were collected giving a total experimental time of 27 h. Data were processed using macros written within the program FELIX95 (MSI Inc., San Diego, CA). Assignments were made by analyzing the TOCSY spectrum in combination with a proton–proton nuclear Overhauser effect spectrum (data not shown). A full assignment and interpretation of the data are underway (P.N.B., H.M., D.A.T and J.W., unpublished observations).

Table 1

Statistics for data collection and model refinement.

Wavelength (Å)	0.98
Resolution (Å)	20–1.6
Reflections (measured/unique)	74,936 (17,338)
a	23.635 Å
b	56.307 Å
c	94.030 Å
Space group	$P2_12_12_1$
Completeness (overall/highest resolution bin)	99.8/100.0 (1.60–1.66 Å)
*R_{scale} (overall/highest resolution bin)	0.043/0.196
$I/\sigma(I)$ (overall/highest resolution bin)	31.8/7.5
†R factor/free R factor	0.167/0.241
‡rmsd: bonds (Å)	0.008
rmsd: angles (degrees)	1.4
Average temp. factor (protein atoms/all atoms, Å2)	19.53/23.75
Number of residues	134
Number of solvent/SO_4^{2-} molecules	215/4

*$R_{scale} = \Sigma|I_n - <I>|/\Sigma<I>$. †R factor $= \Sigma|\{|F_o| - k|F_c|\}|/\Sigma|F_o|$; free R factor $= \Sigma_{(h)\in T}|\{|F_o(\mathbf{h})| - k|F_c(\mathbf{h})|\}|/\Sigma_{(h)\in T}|F_o(\mathbf{h})|$, where T represents a test set of reflections not used in the refinement. ‡rmsd, root mean square deviation.

Crystallization and structure determination of AOP-RANTES

The lyophilized AOP-RANTES sample was resuspended in 10 mM sodium acetate (pH 4.6) at a concentration of 15 mg ml^{-1}. 2 µl of this protein solution was mixed with 2 µl of precipitant [0.1 M ammonium sulfate, 225 mM sodium succinate (pH 4.0), 275 mM 2-(*N*-morpholino)-ethanesulfonic acid (pH 6.0), 15% ethanol]; due to the hydrophobicity of AOP-RANTES, it was further diluted to 20 µl with 16 µl H_2O. This solution was then suspended over 1 ml of the same precipitant and left to equilibrate for 3–4 weeks at 20°C.

Single crystals grew only to a small size ($0.1 \times 0.1 \times 0.05\ mm^3$), as larger crystals became intertwined and were thus unusable. For diffraction experiments, the crystals were mounted on small fiber loops and rapidly cooled in a 100K nitrogen stream, after washing the crystals briefly in the precipitant solution described above (with the addition of 15% glycerol as a cryoprotectant). These small crystals diffracted to only 2.5 Å on a rotating anode X-ray source (Rigaku RU200 generator with a MAR345 image plate), with exposure at a rate of 20 min/degree oscillation. Diffraction extending beyond 1.6 Å, however, was obtained using synchrotron radiation (beamline X9B, NSLS), where a complete data set was collected from a single crystal. The data were collected using 1° oscillations, and individual reflections were integrated and scaled using HKL2000 [35]. Statistics for the data are given in Table 1.

The phases were obtained by molecular replacement using the X-ray structure of Met-RANTES (D.H. and J.L., unpublished observations). Ten percent of the structure amplitudes was then partitioned into a test set to monitor refinement using cross-validation [36]. These data were not used during the refinement. After four rounds of refinement using X-PLOR

[37], the R factor was 0.209 for data in the shell 8–2.4 Å. The refinement was expanded to 1.6 Å resolution, and after seven rounds of refinement and model building, two AOP groups were introduced, and the model included four sulfates, all residues (Pro2–Ser68), and 148 solvents, yielding an R factor of 0.235. After three more rounds, which included both X-PLOR and SHELX-97 [38], the final R factor was 0.167 and the free R factor was 0.241 for the resolution range 20–1.6 Å. Statistics for the refinement and the final model are given in Table 1. The atomic coordinates and structure factors for AOP-RANTES have been deposited with the Protein Data Bank (accession number for the coordinates 1b3a and r1b3asf for experimental structure factors).

Acknowledgements

We thank Lynne Canne and Robin Offord (University of Geneva) for useful discussions. We also thank Zbigniew Dauter (NSLS and SAIC Frederick) for his suggestions on data collection, and Anne Arthur for editorial assistance. This work was supported in part by the AIDS Targeted Antiviral Program of the Office of the Director of the National Institutes of Health to J.L. and A.W. Research sponsored in part by the National Cancer Institute, DHHS, under contract with ABL. The contents of this publication do not necessarily reflect the views or policies of the Department of Health and Human Services, nor does mention of trade names, commercial products or organizations imply endorsement by the U.S. Government.

References

1. Schall, T.J., Bacon, K., Toy, K.J. & Goeddel, D.V. (1990). Selective attraction of monocytes and T lymphocytes of the memory phenotype by cytokine RANTES. *Nature* **347**, 669-671.
2. VanOtteren, G.M., *et al.*, & Standiford, T.J. (1995). Compartmentalized expression of RANTES in a murine model of endotoxemia. *J. Immunol.* **154**, 1900-1908.
3. Robinson, E., Keystone, E.C., Schall, T.J., Gillett, N. & Fish, E.N. (1995). Chemokine expression in rheumatoid arthritis (RA): evidence of RANTES and macrophage inflammatory protein (MIP)-1 beta production by synovial T cells. *Clin. Exp. Immunol.* **101**, 398-407.
4. Gao, J.L., *et al.*, & Murphy, P.M. (1993). Structure and functional expression of the human macrophage inflammatory protein 1 alpha/RANTES receptor. *J. Exp. Med.* **177**, 1421-1427.
5. Neote, K., DiGregorio, D., Mak, J.Y., Horuk, R. & Schall, T.J. (1993). Molecular cloning, functional expression, and signaling characteristics of a C-C chemokine receptor. *Cell* **72**, 415-425.
6. Nomura, H., Nielsen, B.W. & Matsushima, K. (1993). Molecular cloning of cDNAs encoding a LD78 receptor and putative leukocyte chemotactic peptide receptors. *Int. Immunol.* **5**, 1239-1249.
7. Combadiere, C., Ahuja, S.K. & Murphy, P.M. (1995). Cloning and functional expression of a human eosinophil CC chemokine receptor. *J. Biol. Chem.* **270**, 16491-16494.
8. Ben-Baruch, A., Xu, L., Young, P.R., Bengali, K., Oppenheim, J.J. & Wang, J.M. (1995). Monocyte chemotactic protein-3 (MCP3) interacts with multiple leukocyte receptors. C-C CKR1, a receptor for macrophage inflammatory protein-1 alpha/Rantes, is also a functional receptor for MCP3. *J. Biol. Chem.* **270**, 22123-22128.
9. Power, C.A., *et al.*, & Wells, T.N. (1995). Molecular cloning and functional expression of a novel CC chemokine receptor cDNA from a human basophilic cell line. *J. Biol. Chem.* **270**, 19495-19500.
10. Samson, M., Labbe, O., Mollereau, C., Vassart, G. & Parmentier, M. (1996). Molecular cloning and functional expression of a new human CC-chemokine receptor gene. *Biochemistry* **35**, 3362-3367.
11. Raport, C.J., Gosling, J., Schweickart, V.L., Gray, P.W. & Charo, I.F. (1996). Molecular cloning and functional characterization of a novel human CC chemokine receptor (CCR5) for RANTES, MIP-1beta, and MIP-1alpha. *J. Biol. Chem.* **271**, 17161-17166.
12. Combadiere, C., Ahuja, S.K., Tiffany, H.L. & Murphy, P.M. (1996). Cloning and functional expression of CC CKR5, a human monocyte CC chemokine receptor selective for MIP-1(alpha), MIP-1(beta), and RANTES. *J. Leukoc. Biol.* **60**, 147-152.
13. Cocchi, F., DeVico, A.L., Garzino-Demo, A., Arya, S.K., Gallo, R.C. & Lusso, P. (1995). Identification of RANTES, MIP-1 alpha, and MIP-1 beta as the major HIV- suppressive factors produced by CD8+ T cells. *Science* **270**, 1811-1815.
14. Mack, M., *et al.*, & Proudfoot, A.E. (1998). Aminooxypentane-RANTES induces CCR5 internalization but inhibits recycling: a novel inhibitory mechanism of HIV infectivity. *J. Exp. Med.* **187**, 1215-1224.
15. Simmons, G., *et al.*, & Proudfoot, A.E. (1997). Potent inhibition of HIV-1 infectivity in macrophages and lymphocytes by a novel CCR5 antagonist. *Science* **276**, 276-279.
16. Offord, R.E., Gaertner, H.F., Wells, T.N. & Proudfoot, A.E. (1997). Synthesis and evaluation of fluorescent chemokines labeled at the amino terminal. *Methods Enzymol.* **287**, 348-369.
17. Dawson, P.E., Muir, T.W., Clark-Lewis, I. & Kent, S.B. (1994). Synthesis of proteins by native chemical ligation. *Science* **266**, 776-779.
18. Skelton, N.J., Aspiras, F., Ogez, J. & Schall, T.J. (1995). Proton NMR assignments and solution conformation of RANTES, a chemokine of the C-C type. *Biochemistry* **34**, 5329-5342.
19. Chung, C.W., Cooke, R.M., Proudfoot, A.E. & Wells, T.N. (1995). The three-dimensional solution structure of RANTES. *Biochemistry* **34**, 9307-9314.
20. Kent, S.B. (1988). Chemical synthesis of peptides and proteins. *Annu. Rev. Biochem.* **57**, 957-989.
21. Hojo, H. & Aimoto, S. (1991). Polypeptide synthesis using the S-alkyl thioester of a partially protected peptide segment. Synthesis of the DNA-binding domain of c-Myb protein (142-193)-NH_2. *Bull. Chem. Soc. Jpn.* **64**, 111-117.
22. Schnölzer, M., Alewood, P., Jones, A., Alewood, D. & Kent, S.B.H. (1992). *In situ* neutralization in Boc-chemistry solid phase peptide synthesis. *J. Pept. Protein Res.* **40**, 180-193.
23. Dawson, P.E., Churchill, M.J., Ghadiri, M.R. & Kent, S.B.H. (1997). Modulation of reactivity in native chemical ligation through the use of thiol additives. *J. Am. Chem. Soc.* **119**, 4325-4329.
24. Kabsch, W. & Sander, C. (1983). Dictionary of protein secondary structure: pattern of recognition of hydrogen-bonded and geometrical features. *Biopolymers* **22**, 2577-2637.
25. Lubkowski, J., Bujacz, G., Boqué, L., Domaille, P.J., Handel, T.M. & Wlodawer, A. (1997). The structure of MCP-1 in two crystal forms provides a rare example of variable quaternary interactions. *Nat. Struct. Biol.* **4**, 64-69.
26. Hoogewerf, A.J., *et al.*, & Wells, T.N. (1997). Glycosaminoglycans mediate cell surface oligomerization of chemokines. *Biochemistry* **36**, 13570-13578.
27. Pakianathan, D.R., Kuta, E.G., Artis, D.R., Skelton, N.J. & Hebert, C.A. (1997). Distinct but overlapping epitopes for the interaction of a CC-chemokine with CCR1, CCR3 and CCR5. *Biochemistry* **36**, 9642-9648.
28. Gong, J.H., Uguccioni, M., Dewald, B., Baggiolini, M. & Clark-Lewis, I. (1996). RANTES and MCP-3 antagonists bind multiple chemokine receptors. *J. Biol. Chem.* **271**, 10521-10527.
29. Proudfoot, A.E., *et al.*, & Wells, T.N. (1996). Extension of recombinant human RANTES by the retention of the initiating methionine produces a potent antagonist. *J. Biol. Chem.* **271**, 2599-2603.
30. Clark-Lewis, I., *et al.*, & Sykes, B.D. (1995). Structure-activity relationships of chemokines. *J. Leukoc. Biol.* **57**, 703-711.
31. Koopmann, W. & Krangel, M.S. (1997). Identification of a glycosaminoglycan-binding site in chemokine macrophage inflammatory protein-1alpha. *J. Biol. Chem.* **272**, 10103-10109.
32. Laurence, J.S., LiWang, A.C. & LiWang, P.J. (1998). Effect of N-terminal truncation and solution conditions on chemokine dimer stability: nuclear magnetic resonance structural analysis of macrophage inflammatory protein 1 beta mutants. *Biochemistry* **37**, 9346-9354.
33. Shaka, A.J., Shykind, D.N., Chingas, G.C. & Pines, A. (1988). Multiple-pulse sequences for precise transmitter phase alignment. *J. Magn. Res.* **80**, 96-111.
34. Hwang, T.L. & Shaka, A.J. (1995). Water suppression that works - excitation sculpting using arbitrary wave-forms and pulsed-field gradients. *J. Magn. Res.* **112**, 275-279.
35. Otwinowski, Z. & Minor, W. (1997). Processing of X-ray diffraction data collected in oscillation mode. *Methods Enzymol.* **276**, 307-326.
36. Brünger, A.T. & Nilges, M. (1993). Computational challenges for macromolecular structure determination by X-ray crystallography and solution NMR-spectroscopy. *Q. Rev. Biophys.* **26**, 49-125.
37. Brünger, A.T. (1992). *X-PLOR: A System for X-Ray Crystallography and NMR.* Yale University Press, New Haven, CT.
38. Sheldrick, G.M. & Schneider, T.R. (1997). SHELXL: high-resolution refinement. *Methods Enzymol.* **277**, 319-344.
39. Kraulis, P.J. (1991). MOLSCRIPT: a program to produce both detailed and schematic plots of protein structures. *J. Appl. Crystallogr.* **24**, 946-950.
40. Merritt, E.A. & Murphy, M.E.P. (1994). Raster3D version 2.0, a program for photorealistic molecular graphics. *Acta Crystallogr.* **D 50**, 869-873.
41. Carson, M. (1991). RIBBONS 4.0. *J. Appl. Crystallogr.* **24**, 958-961.